



Experimental Estimation of Inertia Tensor and Centre of Gravity of a Mini Helicopter

Kushari A^{1*}, Gupta SK¹, Sharma V¹, Upadhyay CS¹, Venkatesan C¹

¹Department of Aerospace Engineering, Indian Institute of Technology, India

*Corresponding Author: Kushari A, Department of Aerospace Engineering, Indian Institute of Technology, India. E-mail: akushari@iitk.ac.in

Received: 08 May, 2018; Accepted: 18 May, 2018; Published: 05 June, 2018

Abstract

This paper describes the experimental estimation of the mini-helicopter inertia and center of gravity (CG) location. A three degree of freedom inertia test rig and an Inertia Measurement Unit (IMU) were used to measure the oscillation frequencies about three axes under different configurations. These frequency data are then manipulated to estimate the inertia tensor and CG location of the mini-helicopter model.

Keywords: Inertia Estimation; Estimation of Centre of Gravity; Inertia Measurement Scheme

Introduction

Autonomous mini-helicopter is a flying device programmed to accomplish various military and civilian tasks. There are two aspects involved in the development of autonomous mini-helicopters. One aspect is related to the design, and testing of various systems and subsystems and their integration, which is directly related to the hardware. The other aspect involves the analysis and simulation studies which are essential for the evaluation of performance of the complete helicopter system. Therefore it is important to estimate the inertia components and center of gravity location of the helicopter using experimental measurements. It will help us to formulate a theoretical model which can be used in the simulation studies. There has been similar

works reported in the literature [1]. Used nine micro-silicon accelerometers array and its attitude algorithm model to analyze theoretically the strap-down inertia measurement system. The algorithm model is validated by simulation experiment on the ground [2]. Highlights the MAV development which includes system configuration, aerodynamics analysis, prototype fabrication, and flight tests. CG location of the vehicle is estimated. The experimental study to calibrate and compensate the errors of the IMU is presented in [3-9] have reported the results of theoretical and experimental disturbance analysis of a product of inertia measurement system [10]. Have established the importance of the principal axes on the estimates of the inertia tensor [11].

Have proposed a method for reducing

errors in inertia estimates by implementing rotational and translational motions [12]. Have shown that all the rigid body modes of a structure can be extracted using the data from output-only modal analysis. The inertia characteristics and CG location of the helicopter play important role in simulation studies and design of control law. This paper describes a novel experimental technique to estimate these values. It uses frequency response of a 3-D platform with helicopter mounted on it. Least Squares method is used to estimate the inertia and CG location of the mini-helicopter.

Experimental Setup and Measurements

A test rig has been developed to estimate the inertia and CG of the helicopter as shown in (Figure 1) It comprises of outer and inner wooden rectangular frames and an aluminum circular disc. Inner and outer frames rotate about X- and Y-axis respectively, whereas the circular disc rotates about Z-axis. The test rig has a provision to mount the helicopter along the X-axis and its orientation on the rig (in terms of yaw angle) can be changed in steps of 15 degrees each. (Figure 2) shows the helicopter model mounted on the test rig.

The test bed has locking devices to lock any or all oscillatory motions. Three pairs of linear springs are used to limit the motions about the three axes. (Table 1) shows their calibrated spring constant values. These springs are used in pairs to restrict the motion of the test rig to achieve the desired controls (pitch, roll, and yaw). The used spring pairs are tabulated (Table 2).

Figure (1): Photograph of Inertia Measurement Test bed



Figure (2): Helicopter model mounted on the Test Rig



Table (1): Spring constants (N/m) of the springs used in the Test Rig

Spring	Spring Constant K(N/m)
S1	1121.42
S2	1009.03
S3	982.23
S4	1120.79
S5	955.61
S6	1007.27

Table (2): Spring pairs used to restrict the motions of the test rig

Control	Used Spring Pairs	
Yaw (Z-axis)	S3	S5
Pitch (Outer Frame - Y-axis)	S1	S4
Roll (Inner Frame - X-axis)	S2	S6

Whirlybird® digital Inertial Measurement Unit (IMU) was used to measure the frequency of oscillation about these axes. This unit contains two pairs of triad sensors (three accelerometers range of $\pm 2.5g$, three gyroscopes range of ± 250 degree/sec with frame rate 37.5 sample/sec, baud rate 57600 bits per second, and packet format '>' and '\t'). It generates the data via serial port (RS 232) in hexadecimal values. The conversion coefficients are used to convert raw hexadecimal values into acceleration (in m/s^2) and angular rate (degree/sec). The 0.000769 and 0.0152 are the coefficients for accelerometer and rate-gyros respectively. It has built-in low pass filters of 100 Hz each. National Instruments PXI system with an 8 channel PXI 8430 serial module and a developed Lab VIEW program were employed for acquisition, storing and analysis of the data.

Figure (3): Different mounting locations of the helicopter on the test rig

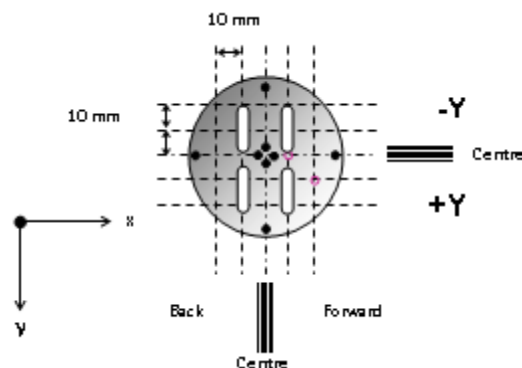
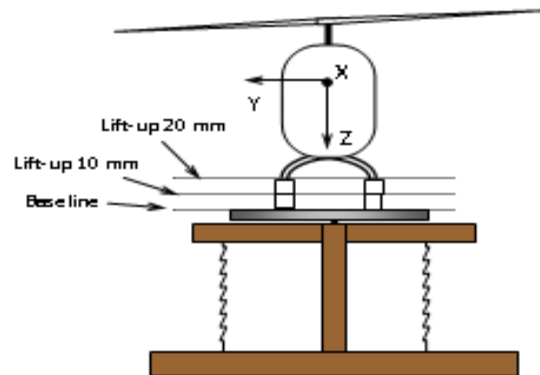


Figure (4): Various lift-up positions on the test rig



Free vibration tests were carried out for the test rig along the three axes (yaw, pitch and roll) with and without mini-helicopter. Initially frequency response of test rig without mini-helicopter was measured with and without added masses of Perspex rectangular rods (used to vary the CG of the mini-helicopter vertically), which is presented in (Table 3). Then frequency response of the test rig with mini-helicopter was measured for different varying CG locations of the mini-helicopter. In the first test, the CG of the mini-helicopter was horizontally shifted on the test rig as shown in (Figure 3) and the obtained frequency response was presented in Table 4.

In the second test, frequency response was obtained for baseline and two lifting-up conditions which is represented in (Figure 4). Yaw orientations of the mini-helicopter on the test rig were also changed from 0 % to 90 % in steps of 15 degrees each. Figures (5,6) shows the yaw orientations of the mini-helicopter with respect to the X-axis. The measured frequency response data is presented in (Table 5). The dynamic data was sampled at 37.5 Hz for duration of 5 seconds. The time response data of the test rig with helicopter under free vibration is presented in (Figure 7). The FFT of the time domain data is presented in (Figure 8). The frequency of the test rig with mini-helicopter at (-10, 20) is found to be 1.608 Hz.

Figure (5): Helicopter mounting at zero yaw orientation

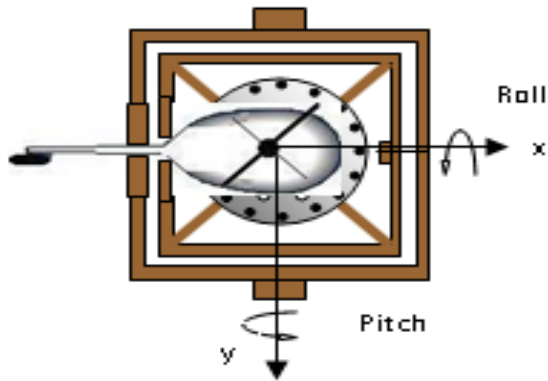


Figure (6): Helicopter mounting at α degree of yaw orientation

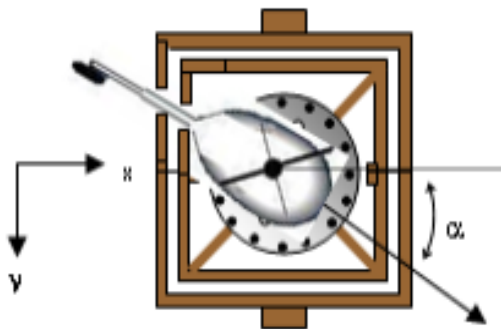


Table (3): Frequency response data of the test rig without the helicopter – Baseline: only test rig response, Lift-up 10 mm and 20 mm: masses of Perspex rods added

	Frequency (Hz)		
	Base-line	Lift-up 10 mm	Lift-up 20 mm
Yaw(Z-axis)	5.825	5.885	5.775
Pitch(Outer Frame Axis-Y axis)	4.042	4.31	4.365
Roll(Inner Frame Axis-X axis)	4.9	4.98	5.02

Table (4): Frequency matrix of the test rig (yaw motion) obtained experimentally with the helicopter

Frequency Measurement f Hz (Yaw Direction)						
Position	Distance	-X Back		Center	+X Forward	
	(mm)	-20	α	0	10	α
	20	1.7	2	2	2	2
+Y	10	1.6	2	2	2	2
Center	0	1.7	2	2	2	2
	-10	1.6	2	2	2	2
-Y	-20	1.7	2	2	2	2

Figure (7): Time response of test rig with mini-helicopter

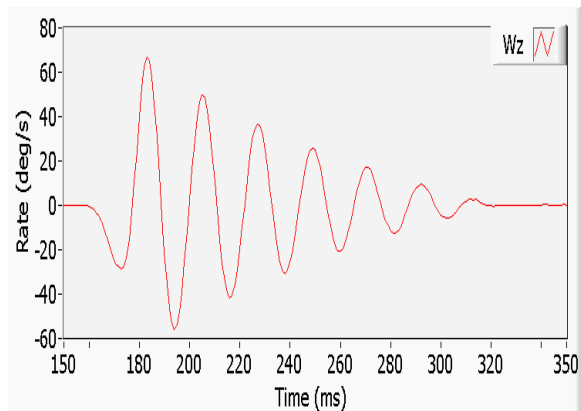


Figure (8): Frequency response obtained from FFT (yaw direction)

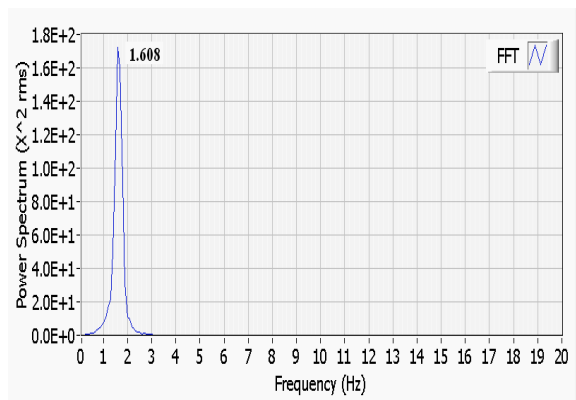


Table (5): Pitch and Roll oscillation frequencies obtained experimentally with the helicopter against different yaw angular and lift-up positions

Yaw Shift angle(Degree)	Frequency f Hz					
	Pitch (Outer Frame, Y-Axis)			Roll (Inner Frame, X-Axis)		
	Baseline	10 mm	20 mm	Baseline	10 mm	20 mm
0	1.708	1.658	1.625	1.855	1.822	1.774
15	1.72	1.685	1.664	1.775	1.767	1.722
30	1.805	1.76	1.71	1.622	1.592	1.592
45	1.928	1.86	1.836	1.465	1.453	1.4
60	2.125	2.01	1.91	1.337	1.327	1.29
75	2.304	2.21	2.127	1.268	1.235	1.247
90	2.422	2.33	2.222	1.243	1.224	1.227

The inertia equations with many unknowns are used to deduce the inertia components and the CG of the helicopter by employing the Least Squares and Newton Raphson methods. These iterative procedures

are used to obtain the best fitted parameters values i.e. inertia tensor and CG location. The following expressions are employed to estimate the inertia tensor and CG location of the mini-helicopter [9]

$$\omega = 2\pi f = \sqrt{\frac{K_{\theta}}{I_{disc}}} \quad \dots (1)$$

$$K_{\theta} = 2 \cdot (r_1^2 \cdot k) \quad \dots (2)$$

$$(I_{ZZ})_{d_est} = \frac{1}{2} m r^2 \quad \dots (3)$$

$$(I_{ZZ})_{hd_est} = \frac{K_{\theta}}{4\pi^2 f_i^2} \quad \dots (4)$$

$$(I_{ZZ})_{hd_est} = (I_{ZZ})_{d_est} + (I_{ZZ})_{heli} + m_{heli} \cdot \left\{ (x_{c.g} + x_i)^2 + (y_{c.g} + y_i)^2 \right\} \quad \dots (5)$$

$$(I_{YY})_{hp_est} = (I_{YY})_{p_est} + (I_{YY})_{heli} + m_{heli} \cdot \left[(Z_{c.g} + h)^2 + X_{c.g}^2 \right] \quad \dots (6)$$

$$(I_{XX})_{hp_est} = (I_{XX})_{p_est} + (I_{XX})_{heli} + m_{heli} \cdot \left[(Z_{c.g} + h)^2 + Y_{c.g}^2 \right] \dots (7)$$

Estimation of Elements of Inertia Tensor and CG Location

The estimated inertia components and CG location of the mini-helicopter are

presented in (Table 6). These values are estimated for a fixed helicopter mass i.e. 5.4 kg. The origin was assumed at the rotor hub and therefore $X_{C.G}$, $Y_{C.G}$, and $Z_{C.G}$ values are manipulated with respect to the rotor hub.

Table (6): Estimated Inertia components and CG location of the mini-helicopter

Quantities	Estimated Values
I_{XX}	0.07043 Kgm ²
I_{YY}	0.15089 Kgm ²
I_{ZZ}	0.17334 Kgm ²
I_{XY}	-0.00274 Kgm ²
$X_{C.G.}$	-0.04828 m
$Y_{C.G.}$	0.01025 m
$Z_{C.G.}$	0.09101 m

Conclusion

The inertia tensor elements and CG location of the helicopter are estimated for oscillation tests carried out on the test rig with and without the helicopter. Yaw, roll and pitch oscillation frequencies are measured against different configurations. These data are processed using Least Squares and Newton-Raphson methods to estimate various inertia components and CG location of the helicopter.

Acknowledgement

Authors would like to express their special thanks to DST, New Delhi for funding the project.

Nomenclature

ω	=	angular velocity, rad/sec
f	=	frequency, Hz
K_{θ}	=	torque stiffness constant, Nm/rad
k	=	spring constant, N/m
m	=	disc mass, kg
r	=	radius of disc, m
$(r_1)_{Z_yaw}$	=	distance of the center of the disc from the spring (Z-axis), m
$(r_1)_{Y_Roll}$	=	distance of the center of the disc from the spring (Y-axis), m
$(r_1)_{X_Pitch}$	=	distance of the center of the disc from the spring (X-axis), m
m_{heli}	=	mass of the helicopter, kg
$(I_{ZZ})_{d_est}$	=	estimated inertia of the disc in Z axis, kgm ²
$(I_{YY})_{p_est}$	=	estimated inertia of the platform in Y axis, kgm ²
$(I_{XX})_{p_est}$	=	estimated inertia of the platform in X axis, kgm ²
$(I_{ZZ})_{hd_est}$	=	estimated Inertia of heli+disc in Z axis, kgm ²
$(I_{YY})_{hp_est}$	=	estimated Inertia of heli+platform in Y axis, kgm ²
$(I_{XX})_{hp_est}$	=	estimated Inertia of heli+platform in X axis, kgm ²

$(I_{ZZ})_{heli}$	=	inertia of the helicopter along Z axis, kgm ²
$(I_{YY})_{heli}$	=	inertia of the helicopter along Y axis, kgm ²
$(I_{XX})_{heli}$	=	inertia of the helicopter along X axis, kgm ²
$(I_{XY})_{heli}$	=	inertia (cross product of X, Y components) of the helicopter, kgm ²
$Z_{c.g.}, Y_{c.g.}, X_{c.g.}$	=	center of gravity of the helicopter, m
(x_i, y_i)	=	i th horizontal mounting location of the helicopter on the test rig for, m
h	=	helicopter height on the platform, m

References

1. Qin L, Zhang W, Zhang H, Xu W (2006) Attitude measurement system based on micro-silicon accelerometer array. *Chaos, Solitons & Fractals*; 29 (1): 141-147.
2. Wu H, Sun D, Zhou Z (2004) Micro Air Vehicle: Configuration, Analysis, Fabrication, and Test. *IEEE/ASME Trans. Mechatronics*; 9(1): 108-117.
3. Ah HS Won CH, Olsen D, et al. (2003) Initial Attitude Estimation of Tactical Grade Inertial Measurement Unit for Airborne Environmental Camera, *Proc. American Control Conf., Colorado*
4. Hung JC, White HV (1975) Self-Alignment Techniques for Inertial Measurement Units. *IEEE Trans. Aerospace and Electronic Systems*. AES; 11(6).
5. Skog I, Handel P (2006) Calibration of a Mems Inertial Measurement Unit. *Proc. XVII IMEKO WORLD CONGRESS Metrology for a Sustainable Development, Brazil*.
6. Hall JJ, Williams RL (2000) Inertial Measurement Unit Calibration Platform. *J. Robotic Systems*; 17(11): 623-632.
7. Hall JJ, Williams R, Frank van Graas (2000) Cartesian Control for the Inertial Measurement Unit Calibration Platform. *Proc. DETC2000 2000 ASME Design Engineering Technical Conference, MD*; 1-8.
8. Kim A, Golnaraghi MF (2004) Initial Calibration of an Inertial Measurement Unit Using an Optical Position Tracking System. *Position Location and Navigation Symposium, PLANS*. 96-101.
9. Fakhari V, Shokrollahi S (2017) A theoretical and experimental disturbance analysis in a product of inertia measurement system. *Measurement*; 107: 142-152.
10. Rossi MM, Alderson J, El-Sallam A, et al. (2016) A new validation technique for estimations of body segment inertia tensors: Principal axes of inertia do matter. *J Biomech*; 49(16): 4119-4123.
11. Barreto JP, Muñoz LE (2016) Low uncertainty method for inertia tensor identification. *Mechanical Systems and Signal Processing*; 68-69: 207-216.
12. Malekjafarian A, Ashory MR, Khatibi MM, et al. (2016) Rigid body stiffness matrix for identification of inertia properties from output-only data. *European Journal of Mechanics - A/Solids*; 59: 85-94.

Citation: Kushari A, et al. (2018) “Experimental Estimation of Inertia Tensor and Centre of Gravity of a Mini Helicopter. J Dyn Mach; 1(1): 1-8.

DOI: [10.31829/2690-0963/dom2018-1\(1\)-103](https://doi.org/10.31829/2690-0963/dom2018-1(1)-103)

Copyright: © 2018 Kushari A, Gupta SK, Sharma V, et al. This is an open-access article distributed under the terms of the Creative Commons Attribution License, which permits unrestricted use, distribution, and reproduction in any medium, provided the original author and source are credited